

# Influence of Cerium (Ce) Doping on the Structural Properties of Silver Telluride ( $\text{Ag}_2\text{Te}$ ) Thin Films Deposited by Electrodeposition Method

<sup>\*1</sup>Lois Ugomma Okafor, <sup>2</sup>Amaechi Okafor Anthony and <sup>3</sup>Sylvester Emeka Abonyi

<sup>1</sup>Department of Physics and industrial physics, Nnamdi Azikiwe University, Awka Anambra State, Nigeria

<sup>2</sup>Department of Mechanical Engineering, Nnamdi Azikiwe University, Awka Anambra State, Nigeria

<sup>3</sup>Department of Electrical Engineering, Nnamdi Azikiwe University, Awka Anambra State, Nigeria

\*Corresponding Author

DOI: <https://dx.doi.org/10.51244/IJRSI.2026.130200103>

Received: 16 February 2026; Accepted: 21 February 2026; Published: 06 March 2026

## ABSTRACT

In this research, Silver Telluride ( $\text{Ag}_2\text{Te}$ ) and Cerium doped Silver Telluride (Ce:  $\text{Ag}_2\text{Te}$ ), thin films have been successfully deposited onto FTO glass substrate using electrodeposition method to investigate the influence of Ce doping on the structural properties of  $\text{Ag}_2\text{Te}$  thin films. Silver trioxonitrate (V) and tellurium (iv) oxide were the precursors used for silver and tellurium ions. Depositions of films made from cerium-doped silver telluride were conducted at room temperature. Variations of structural properties with concentration of cerium dopant, deposition time and with pH were considered in this research. The percentages concentration of cerium dopant used are 5% and 10.0%. The Structural properties of  $\text{Ag}_2\text{Te}$  and Ce doped  $\text{Ag}_2\text{Te}$  thin films were investigated using X-ray diffractometry. The structural properties analysis of pure  $\text{Ag}_2\text{Te}$  and cerium-doped  $\text{Ag}_2\text{Te}$  thin films reveals significant changes in crystallographic properties (crystallite size, micro-strain and dislocation density) with increasing cerium concentration. The increase in crystallite size, coupled with the decrease in micro-strain and dislocation density, suggests that cerium doping improves the structural quality of  $\text{Ag}_2\text{Te}$  thin films, potentially enhancing their properties. The higher intensities of the doped samples' diffraction peaks imply better crystallinity and possibly lower defect densities, which are beneficial for applications requiring high-quality crystalline materials. Longer deposition times and optimizing pH enhance crystallinity, where lower values generally improve crystal quality by reducing lattice distortions. The findings highlight how controlled doping, deposition time, and pH conditions can fine-tune the structural properties of cerium doped silver telluride thin films, making it suitable for applications in optoelectronics and electronic devices.

**Keywords:** Silver-Telluride, Structural properties, Electrodeposition, X-ray diffractometer machine

## INTRODUCTION

Silver telluride ( $\text{Ag}_2\text{Te}$ ) is a chalcogenide semiconductor composed of silver (Ag) and tellurium (Te), belonging to group iv-vi compounds on the periodic table [1] which exhibit semiconductor properties. In bulk form, it crystallizes in a monoclinic  $\beta$  – phase at room temperature and undergoes a phase transition to a cubic  $\alpha$  – phase at elevated temperatures, approximately 423K [2], with associated changes in electrical behavior.  $\text{Ag}_2\text{Te}$  exhibits n-type conductivity and has been studied for magneto resistance and thermo electric applications [2]. Nanostructured forms of silver telluride, such as quantum dots or nanorods, show enhanced properties due to quantum confinement effects, including increased band gaps and strong photoluminescence within infrared range, which differs greatly from bulk materials [3]. These nanostructures are synthesized by different methods such as hydrothermal processes or chemical deposition, using precursors such as  $\text{AgNO}_3$  and  $\text{TeCl}_4$  [4]. Recently,  $\text{Ag}_2\text{Te}$  quantum dots have emerged as heavy metal-free alternatives to traditional chalcogenide nano materials, giving tunable optoelectronic properties for near-infrared (NR) and shortwave infrared (SWIR) photodetectors

with competitive responsivity and detectivity [3]. Besides optoelectronics, the compound finds application in non linear optical devices, ion-selective electrodes, electrochemical storage cells, solar cells and biological sensors, stating its versatility in energy, environmental and sensing technologies [2]. Reports from literature [6, 7, 8, 9] showed no information on the influence of dopant concentration, deposition time and pH on the structural properties of cerium doped silver telluride films. The purpose of this research is to address the literature gap by investigating the influence of concentration of cerium doping, deposition time and pH on the structural properties of silver telluride films synthesized via electrodeposition.

## Experimental

### Reagents

Reagents used for electrodeposition of cerium doped silver telluride ( $Ce:AgTe$ ) were; Silver nitrate : used as precursor for silver ion., Cerium (iv) sulfate tetrahydrate: used as precursor for cerium ion (dopant ion), Tellurium (IV) oxide: used as precursor for tellurium ion, ethylene diamine tetra acetic acid (EDTA): used as a complexing agent, distilled water was used as solvent.

### Apparatus

The experimental arrangement shown in section 3.5, Figure 1 [5] illustrates the setup for electrodeposition, comprising the electrolyte, power supply unit, and electrodes. It adopts a three-electrode configuration for depositing thin films onto conducting substrates. The conducting substrate, specifically FTO, was used as the cathode or working electrode. A platinum electrode functioned as the anode or counter electrode, while a silver/silver chloride (Ag/AgCl) electrode served as the reference electrode. The energy supply for the electrodeposition setup is provided by a Dazheng digital DC-power supply unit, specifically the PS-1502A model. Two digital multimeters, the DT9201A CE and the highly sensitive Mastech: MY60 were employed for measuring voltage and current, respectively. The Mastech: MY60 multimeter is capable of measuring currents within the range of  $10^{-6}$  A.

### Material preparation

Molar solutions of the reagents prepared for the deposition include:

#### Silver nitrate

Silver nitrate is an inorganic compound with chemical formula  $AgNO_3$ . It is a versatile precursor to many other silver compounds. It is a colorless salt with molar mass of 169.87 g/mol. About 256 g of the salt is soluble in 100 ml at 25 °C. In this work, silver nitrate served as precursor for Ag ion and various concentrations (0.10 M and 0.01 M) of silver nitrate was prepared by dissolving particular amount of the compound in 100 ml of distilled water.

#### Cerium (iv) sulfate tetrahydrate

Cerium (IV) sulfate tetrahydrate, also called ceric sulfate, is an inorganic compound with chemical formula  $(Ce(SO_4)_2 \cdot 4H_2O)$ . The salt is a yellow solids that are moderately soluble in water and dilute acids. Solutions of ceric sulfate have a strong yellow color. It has a molar mass of 404.30 g/mol. In this work, 0.01 M of the salt was prepared by dissolving 0.40 g in 100 ml of distilled water

#### Tellurium (IV) oxide

Tellurium (IV) oxide, also known as tellurium dioxide ( $TeO_2$ ) is a white crystalline solid with molecular weight of 159.60 g/mol and it is negligible soluble in water. Tellurium (IV) oxide served as precursor for tellurium ion. In this work, 0.20 mole solution of  $TeO_2$  was prepared by dissolving 7.98 g in 250 ml of distilled water.

## Diluted sulfuric acid solution

H<sub>2</sub>SO<sub>4</sub> has a molar mass of 98.079 g/mol. 1.0 M of H<sub>2</sub>SO<sub>4</sub> was prepared by adding 55.60 ml of 96 % concentrated H<sub>2</sub>SO<sub>4</sub> to 1000 ml of distilled water. The 55.60 ml of H<sub>2</sub>SO<sub>4</sub> was obtained by using the percentage concentration of the H<sub>2</sub>SO<sub>4</sub> (96%), molar mass of H<sub>2</sub>SO<sub>4</sub> (98.079 g/mol) and specific density of (1.84 g/ml). The diluted H<sub>2</sub>SO<sub>4</sub> served as pH adjuster

## Substrate pre-treatment

Prior to electrodeposition of the films, the FTO substrates were subjected to distinct pre – treatment to ensure the presence of catalytic surface to improve the adhesion of the films to the substrates most especially when there is possibility of increase in film thickness as deposition proceeds. This pre – treatment of FTO glass substrates was achieved through the following six steps;

- (i) We cleaned the FTO glass substrates with detergents.
- (ii) We soaked the substrates in acetone for 10 minutes for degreasing.
- (iii) We ultrasonicated the substrates for 20 minutes in an ultrasonic bath using ethanol as a solvent.
- (iv) We ultrasonicated the substrates for 10 minutes in an ultrasonic bath using distilled as a solvent.
- (v) We rinsed the substrates twice with distilled water.
- (vi) We dried the substrates in an electronic oven for 10 minutes at a temperature of about 100°C.

## Electrodeposition

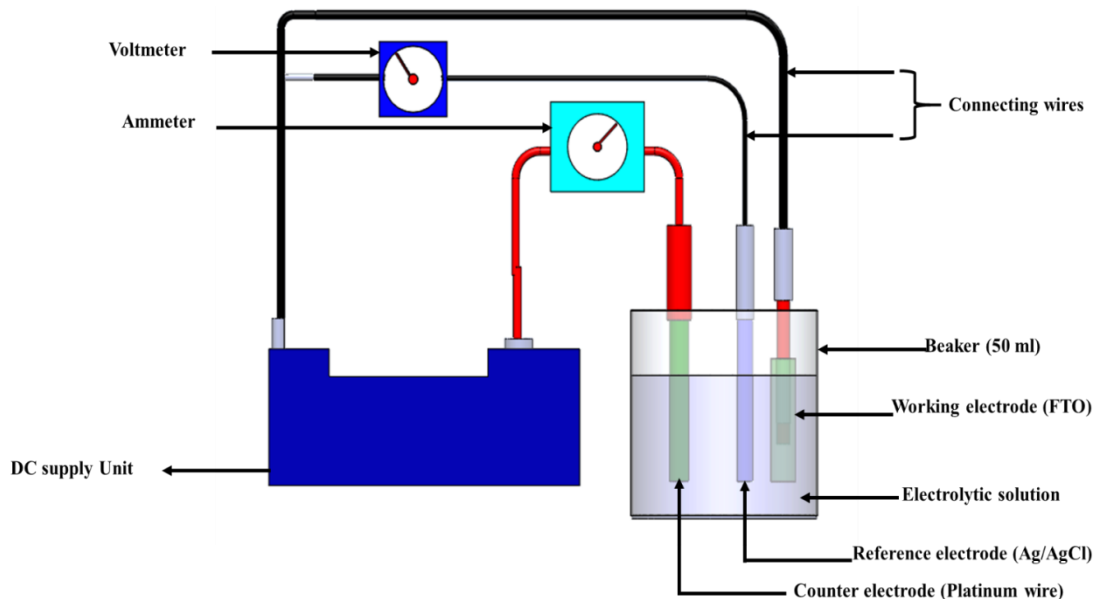


Figure 1: Schematic diagram of the electrodeposition experimental set – up [5]

Depositions of thin films made from cerium-doped silver chalcogenide ( Ce:Ag<sub>2</sub>Te) were conducted at room temperature. Molar concentration bath parameter of the cerium precursor was adjusted to optimize their impact on the optical characteristics of these films.

## Electrodeposition of silver telluride and cerium doped silver telluride (Ce: Ag<sub>2</sub>Te) thin films

For electrodeposition of silver telluride thin film on FTO substrate, aqueous electrolytic bath composed of 20 ml of 0.10 M of silver trioxonitrate (V) and 5 ml of 1.0 M of H<sub>2</sub>SO<sub>4</sub> were poured into the electrolytic bath. The

mixture was stirred for 5 minutes. This was followed by addition of 15 ml of 0.1 M of tellurium (IV) oxide solution to the mixture. This followed with another stirring for 5 minutes. After stirring, the three electrodes were immersed into the bath containing the electrolytic solution and 2 volts was allowed to pass through the setup for 15 seconds. After the allowed time, grey film of Ag<sub>2</sub>Te was found to be deposited on the conductive surface of the FTO substrate. The deposited Ag<sub>2</sub>Te thin film was heat-treated at 100 °C for 10 minute to remove water and improve the crystallinity of the deposited thin films. The mechanism of the formation of silver telluride and cerium doped silver telluride is shown in equation (1) and (2).



**Optimization of Ce ion concentration for Ce: Ag<sub>2</sub>Te thin films**

For the deposition of Ce doped Ag<sub>2</sub>Te thin films, 0.05 M of cerium (IV) sulfate tetrahydrate was used as dopant source. Similar procedure used for deposition of silver telluride thin film was adopted but with addition of different volume concentrations of 0.05 M of cerium (IV) sulfate tetrahydrate as shown in Table 1. Four samples with different dopant volume concentrations of 1 ml, 2 ml, 3 ml and 4 ml were fabricated.

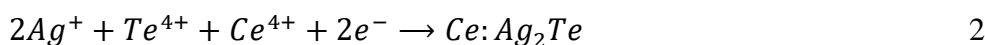


Table 1: Bath parameter for deposition of Ag<sub>2</sub>Te and Ce doped Ag<sub>2</sub>Te thin films

0.10 M of AgNO <sub>3</sub>	0.10 M of TeO <sub>2</sub>	0.05 M of CeSO <sub>4</sub> ·4H <sub>2</sub> O	1.0 M of H <sub>2</sub> SO <sub>4</sub>	Applied Voltage	Time
Vol. (ml)	Vol. (ml)	Vol. (ml)	Vol. (ml)	(volts)	(sec.)
20.00	15.00	-	5.00	2.00	15
20.00	15.00	1.00	5.00	2.00	15
20.00	15.00	2.00	5.00	2.00	15
20.00	15.00	3.00	5.00	2.00	15
20.00	15.00	4.00	5.00	2.00	15

**Optimization of deposition time for Ce: Ag<sub>2</sub>Te thin films**

For time optimization of Ce doped Ag<sub>2</sub>Te thin films, similar procedure used for deposition of cerium doped silver telluride thin film was adopted. 0.10 M of silver nitrate, 1.0 M of H<sub>2</sub>SO<sub>4</sub>, 0.1 M of tellurium (IV) oxide and 0.05 M of cerium (IV) sulfate tetrahydrate were used to deposit the desired thin film. Five films were deposited at time interval of 10 seconds, 20 seconds, 30 seconds, 40 seconds and 50 seconds. Table 3.8 shows the constituent of the electrolytic baths used for the deposition of Ce doped Ag<sub>2</sub>Te at varying deposition time.

Table 2: Bath parameter for time optimized Ce: Ag<sub>2</sub>Te thin films

0.10 M of AgNO <sub>3</sub>	0.10 M of TeO <sub>2</sub>	0.05 M of CeSO <sub>4</sub> ·4H <sub>2</sub> O	1.0 M of H <sub>2</sub> SO <sub>4</sub>	Applied Voltage	Time
Vol. (ml)	Vol. (ml)	Vol. (ml)	Vol. (ml)	(volts)	(sec.)
20.00	15.00	2.00	5.00	2.00	10
20.00	15.00	2.00	5.00	2.00	20

20.00	15.00	2.00	5.00	2.00	30
20.00	15.00	2.00	5.00	2.00	40
20.00	15.00	2.00	5.00	2.00	50

**Optimization of deposition pH for Ce: Ag<sub>2</sub>Te thin films**

For pH optimization of Ce doped Ag<sub>2</sub>Te thin films, similar procedures used for deposition of cerium doped silver telluride thin film were maintained. The 0.10 M of silver nitrate, 1.0 M of H<sub>2</sub>SO<sub>4</sub>, 0.10 M of tellurium (IV) oxide and 0.05 M of cerium (IV) sulfate tetrahydrate were used for the deposition of Ce doped Ag<sub>2</sub>Te thin films at varying pH. Five films were deposited with different volume concentration of H<sub>2</sub>SO<sub>4</sub>. 1 ml, 2 ml, 3 ml, 4 ml and 5 ml of H<sub>2</sub>SO<sub>4</sub> were used to achieve variation in pH of the medium. Table 3.9 shows the constituent of the electrolytic baths used for the deposition of Ce doped Ag<sub>2</sub>Te at varying pH.

Table 3: Bath parameter for pH optimized Ce: Ag<sub>2</sub>Te thin films

0.10 M of AgNO <sub>3</sub>	0.10 M of TeO <sub>2</sub>	0.05 M of CeSO <sub>4</sub> ·4H <sub>2</sub> O	1.0 M of H <sub>2</sub> SO <sub>4</sub>	Applied Voltage	Time
Vol. (ml)	Vol. (ml)	Vol. (ml)	Vol. (ml)	(volts)	(sec.)
20.00	15.00	2.00	1.00	2.00	15
20.00	15.00	2.00	2.00	2.00	15
20.00	15.00	2.00	3.00	2.00	15
20.00	15.00	2.00	4.00	2.00	15
20.00	15.00	2.00	5.00	2.00	15

**Characterization of deposited thin films**

The fabricated thin films were characterized to determine their optical properties using spectrophotometer, Thickness measurements of the films were carried out using gravimetric method

**Film thickness measurement**

The deposited film thicknesses (t) were evaluated using the gravimetric method given by [10]; [11]; [12].

$$t = \frac{\Delta m}{\rho A}, \tag{3}$$

In equation (3), Δm is the mass of the film. A is the surface area of the deposited film and ρ is the bulk density of the material film. The masses of the deposited films were obtained by finding the difference in mass between the mass of the glass substrate with the film after deposited and the mass of glass substrate before deposition. These differences in mass of the films were measured using analytical weighing balance with sensitivity of 0.0001 g.

Bulk density of Ag<sub>2</sub>Te is 8.32 g/cm<sup>3</sup>. Bulk density of cerium is 8.16 g/cm<sup>3</sup>. Because of small amount of cerium impurity used and possibility of cerium ions to substitute silver in the crystal structure, density of Ce:Ag<sub>2</sub>Te was approximated to bulk density of Ag<sub>2</sub>Te

## Structural characterization

Crystal structural analyses of the deposited thin films were done using x – ray diffractometer machine. From the x – ray diffraction pattern obtained, other structural properties such as d – spacing, full width at half maximum (FWHM) were obtained. The crystallite sizes and microstrains of the films were evaluated using Scherrer’s formula. Debye – Scherrer’s formula for calculating crystallite sizes of a thin film material is given by [13; 14] as

$$D = \frac{0.9 \lambda}{\beta \cos \theta} \tag{4}$$

The dislocation density ( $\delta$ ) of thin films can be estimated using expression as provided by [15; 16] in equation (5).

$$\delta = \frac{1}{D^2} \tag{5}$$

Micro-strain ( $\epsilon$ ) of thin film sample can be estimated using the expression in equation (6) as given by [17 and 18].

$$\epsilon = \frac{\beta}{4 \tan \theta} \tag{6}$$

## RESULTS AND DISCUSSIONS

### Structural properties of Ag<sub>2</sub>Te and Ce doped Ag<sub>2</sub>Te thin films

#### (a) Variation of structural properties with concentration of cerium dopant

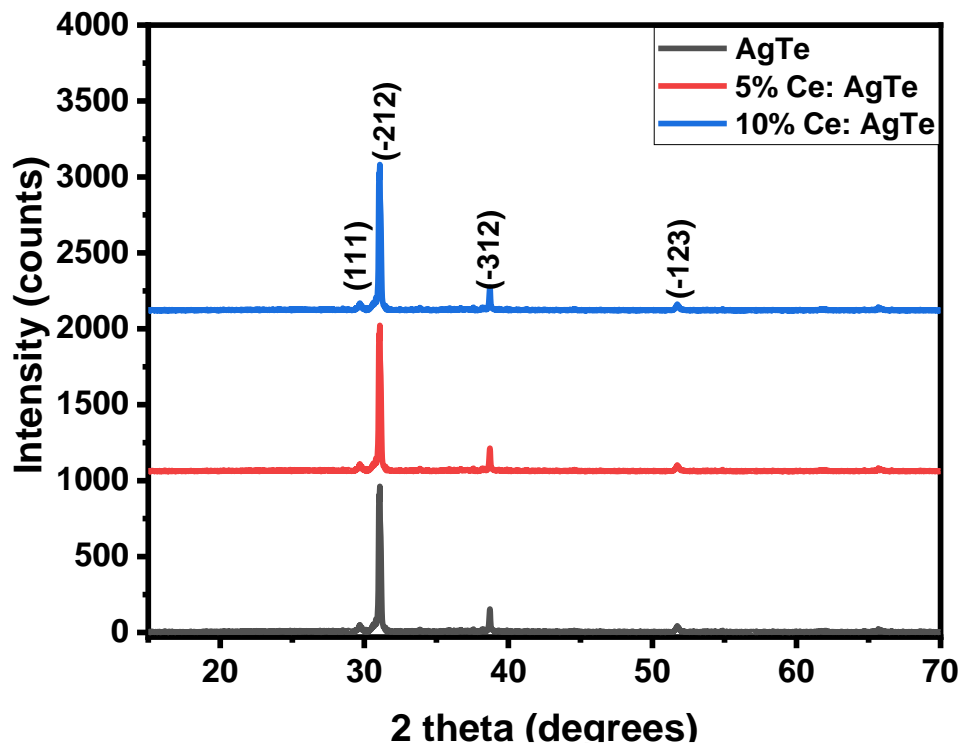


Figure 2: Diffractogram of Ag<sub>2</sub>Te and cerium doped Ag<sub>2</sub>Te deposited with different percentage concentration of dopant

Figure 2 shows the diffractogram of Ag<sub>2</sub>Te and cerium doped Ag<sub>2</sub>Te thin films deposited at different concentration of cerium ion. The diffractogram and accompanying table provide insight into the structural parameters of Ag<sub>2</sub>Te and cerium-doped Ag<sub>2</sub>Te thin films, with Ag<sub>2</sub>Te corresponding to the JCPDS file number 01-081-1985 and known mineralogically as Hessite. The XRD patterns reveal distinct peaks corresponding to

various crystallographic planes, indicating the monoclinic phase of Ag<sub>2</sub>Te. The intensity of the diffraction peaks varies with the doping concentration, with undoped Ag<sub>2</sub>Te showing lower peak intensities compared to the cerium-doped samples.

Table 4: Structural parameters of Ag<sub>2</sub>Te and cerium doped Ag<sub>2</sub>Te thin films

Doping Level	2 Theta (°)	hkl	FWHM (°)	Crystallite Size (nm)	Dislocation Density × 10 <sup>-3</sup> lines/nm <sup>2</sup>	Micro-strain (ε) × 10 <sup>-3</sup>
Ag <sub>2</sub> Te	33.827	111	0.305	28.142	1.263	5.019
	39.996	-212	0.187	46.041	0.472	2.936
	43.422	-312	0.113	78.151	0.164	1.398
	<b>Average</b>			<b>50.778</b>	<b>0.633</b>	<b>3.118</b>
5% Ce: Ag <sub>2</sub> Te	29.706	111	0.277	31.014	1.040	4.554
	31.065	-212	0.187	46.031	0.472	2.937
	38.710	-312	0.113	77.992	0.164	1.401
	51.733	-123	0.274	33.596	0.886	2.470
	<b>Average</b>			<b>51.679</b>	<b>0.559</b>	<b>2.964</b>
10% Ce: Ag <sub>2</sub> Te	30.731	111	0.216	39.764	0.632	3.436
	31.065	-212	0.161	53.586	0.348	2.523
	38.710	-312	0.113	77.518	0.166	1.409
	51.733	-123	0.221	41.736	0.574	1.988
	<b>Average</b>			<b>53.151</b>	<b>0.430</b>	<b>2.339</b>

Specifically, the intensity for the (111) plane increases significantly with 10% Ce doping, indicating enhanced crystallinity and possibly higher atomic density in these planes. Analysis shows that undoped Ag<sub>2</sub>Te has crystallite sizes ranging from 28.142 nm to 78.151 nm, dislocation densities from 0.164 × 10<sup>-3</sup> lines/nm<sup>2</sup> to 1.263 × 10<sup>-3</sup> lines/nm<sup>2</sup>, and micro-strain from 1.398 × 10<sup>-3</sup> to 5.019 × 10<sup>-3</sup>. With 5% Ce doping, the crystallite sizes range from 31.014 nm to 77.992 nm, dislocation densities from 0.164 × 10<sup>-3</sup> lines/nm<sup>2</sup> to 1.040 × 10<sup>-3</sup> lines/nm<sup>2</sup>, and micro-strain from 1.401 × 10<sup>-3</sup> to 4.554 × 10<sup>-3</sup>. For 10% Ce doping, the crystallite sizes range from 39.764 nm to 77.518 nm, dislocation densities from 0.166 × 10<sup>-3</sup> lines/nm<sup>2</sup> to 0.632 × 10<sup>-3</sup> lines/nm<sup>2</sup>, and dislocation densities from 1.409 × 10<sup>-3</sup> to 3.436 × 10<sup>-3</sup> lines/nm<sup>2</sup>. Analysis shows that undoped Ag<sub>2</sub>Te has an average crystallite size of 50.778 nm, dislocation density of 0.633 × 10<sup>-3</sup> lines/nm<sup>2</sup> and micro-strain of 3.118 × 10<sup>-3</sup> lines/nm<sup>2</sup>. With 5% Ce doping, these parameters improve to 51.679 nm, 0.559 × 10<sup>-3</sup> lines/nm<sup>2</sup>, and 2.964 × 10<sup>-3</sup>, respectively. Further enhancement is observed with 10% Ce doping, resulting in an average crystallite size of 53.151 nm, dislocation density of 0.430 × 10<sup>-3</sup> and micro-strain of 2.339 × 10<sup>-3</sup>. The increase in crystallite size, coupled with the decrease in micro-strain and dislocation density, suggests that cerium doping improves the structural quality of Ag<sub>2</sub>Te thin films, potentially enhancing their properties. The higher intensities of the doped samples' diffraction peaks imply better crystallinity and possibly lower defect densities, which are beneficial for applications requiring high-quality crystalline materials.

(b) Variation of structural properties with deposition time

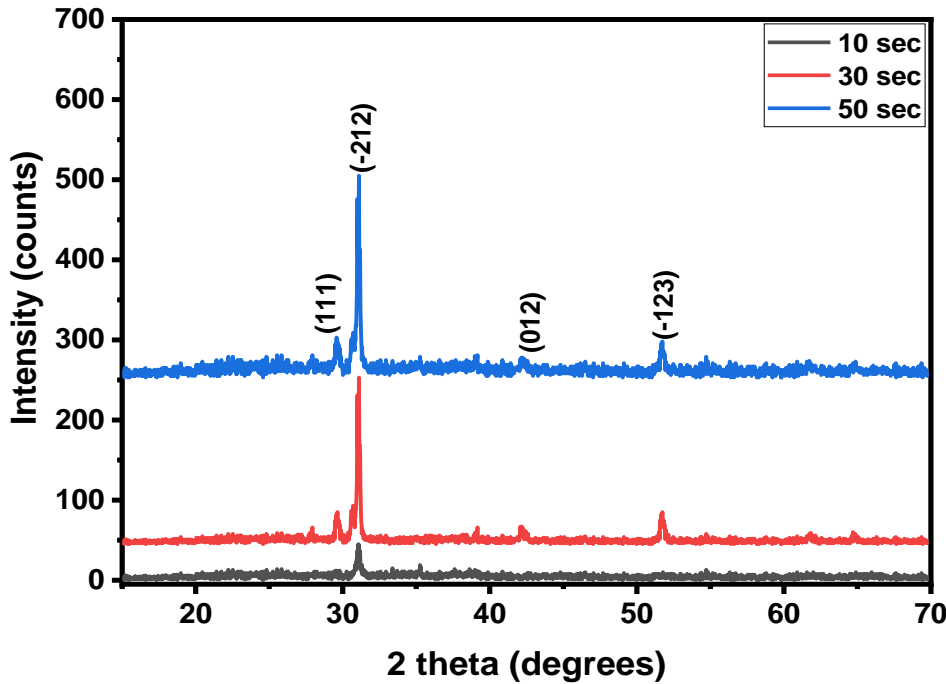


Figure 3: Diffractogram of cerium doped Ag<sub>2</sub>Te deposited under different deposition time

Figure 3 shows the diffractogram of cerium doped silver telluride thin films deposited at different time of deposition. The diffractogram in figure 3 and table 5 provide detailed insights into the structural parameters of cerium-doped Ag<sub>2</sub>Te thin films deposited under different deposition times. The deposited cerium doped Ag<sub>2</sub>Te corresponding to the JCPDS file number 01-081-1985 and known mineralogically as Hessite. The XRD patterns reveal distinct peaks corresponding to various crystallographic planes, indicating the monoclinic phase of Ag<sub>2</sub>Te. The intensity of the diffraction peaks varies with the deposition time, with longer deposition times resulting in higher peak intensities, suggesting improved crystallinity. Specifically, the (-212) plane shows a significant increase in intensity with increased deposition time, indicating enhanced atomic density in these planes.

Table 5: Structural parameters of cerium doped Ag<sub>2</sub>Te thin films deposited at different time

Doping Level	2 Theta (°)	hkl	FWHM (°)	Crystallite Size (nm)	Dislocation Density × 10 <sup>-3</sup> lines/nm <sup>2</sup>	Micro-strain (ε) × 10 <sup>-3</sup>
10 seconds	31.065	-212	0.217	39.677	0.635	3.407
	<b>Average</b>			<b>39.677</b>	<b>0.635</b>	<b>3.407</b>
30 seconds	29.622	111	0.229	37.534	0.710	3.773
	31.068	-212	0.146	58.994	0.287	2.292
	42.225	-312	0.271	32.873	0.925	3.058
	51.722	-123	0.212	43.574	0.527	1.905
	<b>Average</b>			<b>43.244</b>	<b>0.612</b>	<b>2.757</b>
50 seconds	29.620	111	0.211	40.652	0.605	3.484

	31.067	-212	0.156	55.272	0.327	2.446
	42.244	-312	0.240	37.044	0.729	2.712
	51.724	-123	0.203	45.486	0.483	1.825
	<b>Average</b>			<b>44.613</b>	<b>0.536</b>	<b>2.617</b>

For the 10-second deposition time, the average crystallite size is 39.677 nm, dislocation density is  $0.635 \times 10^{-3}$  lines/nm<sup>2</sup>, and micro-strain is  $3.407 \times 10^{-3}$ . For the 30-second deposition time, the crystallite sizes range from 32.873 nm to 58.994 nm, dislocation densities from  $0.287 \times 10^{-3}$  to  $0.925 \times 10^{-3}$  lines/nm<sup>2</sup>, and micro-strain values from  $1.905 \times 10^{-3}$  to  $3.773 \times 10^{-3}$ , with an average crystallite size of 43.244 nm, dislocation density of  $0.612 \times 10^{-3}$  lines/nm<sup>2</sup>, and micro-strain of  $2.757 \times 10^{-3}$ . For the 50-second deposition time, the crystallite sizes range from 37.044 nm to 55.272 nm, dislocation densities from  $0.327 \times 10^{-3}$  to  $0.729 \times 10^{-3}$  lines/nm<sup>2</sup>, and micro-strain values from  $1.825 \times 10^{-3}$  to  $3.484 \times 10^{-3}$ , with an average crystallite size of 44.613 nm, dislocation density of  $0.536 \times 10^{-3}$  lines/nm<sup>2</sup>, and micro-strain of  $2.617 \times 10^{-3}$ .

The table indicates that increased deposition time enhances the structural quality of cerium-doped Ag<sub>2</sub>Te thin films by increasing crystallite size, reducing dislocation density, and lowering micro-strain. The higher intensities of the diffraction peaks with longer deposition times imply better crystallinity and potentially lower defect densities, which are beneficial for applications requiring high-quality crystalline materials.

(c) Variation of structural properties with pH

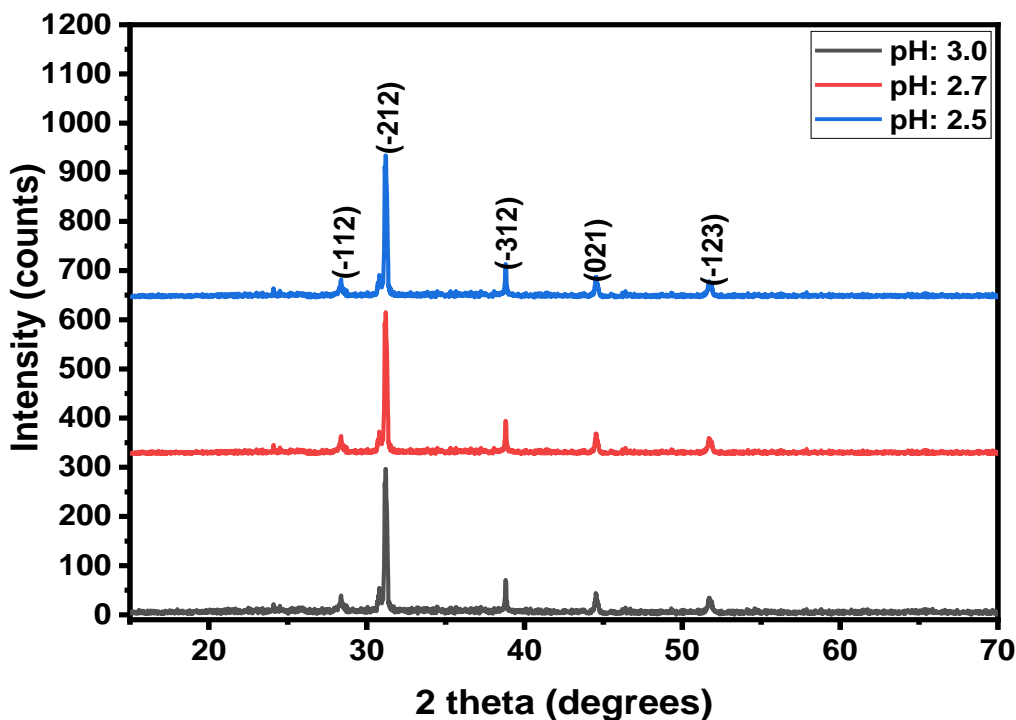


Figure 4: Diffractogram of cerium doped Ag<sub>2</sub>Te deposited under different pH value

The diffractogram as shown in Figure 4 and the structural parameters in table 6 provide detailed insights into the structural quality of cerium-doped Ag<sub>2</sub>Te thin films deposited under different pH conditions. Ag<sub>2</sub>Te corresponds to the JCPDS file number 01-081-1985 and is known mineralogically as Hessite. The XRD patterns reveal distinct peaks corresponding to various crystallographic planes, indicating the monoclinic phase of Ag<sub>2</sub>Te. The intensity of the diffraction peaks varies with the pH value of the deposition solution, higher pH values results in lower peak intensities, suggests improved crystallinity. Specifically, the intensity of the (-212) plane shows a significant increase with higher pH, indicating enhanced atomic density in these planes.

Table 6: Structural parameters of cerium doped Ag<sub>2</sub>Te thin films deposited at different pH

pH	2 Theta (°)	hkl	FWHM (°)	Crystallite Size (nm)	Dislocation Density × 10 <sup>-3</sup> lines/nm <sup>2</sup>	Micro-strain (ε) × 10 <sup>-3</sup>
3.0	28.383	-112	0.386	22.163	2.036	6.663
	31.208	-212	0.197	43.746	0.523	3.077
	38.809	-312	0.111	79.324	0.159	1.374
	44.548	021	0.220	40.740	0.603	2.345
	51.741	-123	0.283	32.623	0.940	2.543
	<b>Average</b>			<b>48.411</b>	<b>0.906</b>	<b>3.705</b>
2.7	28.376	-112	0.309	27.740	1.300	5.325
	31.208	-212	0.196	43.935	0.518	3.063
	38.809	-312	0.113	77.548	0.166	1.405
	44.550	021	0.226	39.601	0.638	2.412
	51.743	-123	0.295	31.248	1.024	2.655
		<b>Average</b>			<b>49.741</b>	<b>0.661</b>
2.5	28.376	-112	0.209	41.040	0.594	3.599
	31.208	-212	0.196	43.935	0.518	3.063
	38.809	-312	0.113	77.548	0.166	1.405
	44.550	021	0.226	39.601	0.638	2.412
	51.743	-123	0.295	31.248	1.024	2.655
<b>Average</b>				<b>50.531</b>	<b>0.479</b>	<b>2.620</b>

For the pH 3.0 deposition, the crystallite sizes range from 22.163 nm to 79.324 nm, dislocation densities from  $0.159 \times 10^{-3}$  to  $2.036 \times 10^{-3}$  lines/nm<sup>2</sup>, and micro-strain values from  $1.374 \times 10^{-3}$  to  $6.663 \times 10^{-3}$ , with an average crystallite size of 48.411 nm, dislocation density of  $0.906 \times 10^{-3}$  lines/nm<sup>2</sup>, and micro-strain of  $3.705 \times 10^{-3}$ . For the pH 2.7 deposition, the crystallite sizes range from 27.740 nm to 77.548 nm, dislocation densities from  $0.166 \times 10^{-3}$  to  $1.300 \times 10^{-3}$  lines/nm<sup>2</sup>, and micro-strain values from  $1.405 \times 10^{-3}$  to  $5.325 \times 10^{-3}$ , with an average crystallite size of 49.741 nm, dislocation density of  $0.661 \times 10^{-3}$  lines/nm<sup>2</sup>, and micro-strain of  $3.264 \times 10^{-3}$ . For the pH 2.5 deposition, the crystallite sizes range from 31.248 nm to 77.548 nm, dislocation densities from  $0.166 \times 10^{-3}$  to  $1.024 \times 10^{-3}$  lines/nm<sup>2</sup>, and micro-strain values from  $1.405 \times 10^{-3}$  to  $3.599 \times 10^{-3}$ , with an average crystallite size of 50.531 nm, dislocation density of  $0.479 \times 10^{-3}$  lines/nm<sup>2</sup>, and micro-strain of  $2.620 \times 10^{-3}$ . The results as shown in table 4.9 indicate that higher pH values reduces the structural quality of cerium-doped Ag<sub>2</sub>Te thin films by decreasing crystallite size, reducing dislocation density, and lowering micro-strain. The lower intensities of the diffraction peaks with lower pH values imply better crystallinity and potentially lower defect densities, which are beneficial for applications requiring high-quality crystalline materials.

## CONCLUSION

Thin films of silver telluride ( $\text{Ag}_2\text{Te}$ ), and cerium-doped silver telluride ( $\text{Ce: Ag}_2\text{Te}$ ) were successfully deposited on fluorine-doped tin oxide (FTO) glass substrates using the electrodeposition technique. The precursors used for the deposition included aqueous solutions of silver trioxonitrate (V), cerium tetraoxosulphate (VI) tetrahydrate, and tellurium (IV) oxide, which served as sources of Ag, Ce, and Te, respectively. Ethylene diamine tetra acetic acid (EDTA) was employed as a complexing agent, while tetraoxosulphate (VI) acid was used to adjust the pH of the electrolyte bath. Cerium ions were incorporated as dopants into  $\text{Ag}_2\text{Te}$  matrices. Deposition parameter such as dopant concentration (5% and 10%), pH and time were systematically optimized to study their effects on the film structural properties.

Structural properties obtained from X-ray diffraction (XRD) revealed that  $\text{Ag}_2\text{Te}$  crystallized in the monoclinic phase. Cerium doping led to enhanced peak intensities and reduced peak broadening, indicating improved crystallinity. Crystallite sizes increased with doping and optimized deposition parameters: from 39.68 to 53.15 nm. Dislocation densities correspondingly decreased from  $0.91 \times 10^{-3}$  to  $0.43 \times 10^{-3}$  while micro-strain values also reduced, confirming enhanced crystal quality.

## REFERENCES

1. Nande, A., Kalyani, N. T., Tiwari, A., Dhoble, S. J. Exploring the world of functional materials. In Functional Materials from Carbon, Inorganic, and Organic Sources Woodhead Publishing Series in Electronic and Optical Materials, Woodhead Publishing, 2023, pp 1-19
2. Sousan Gholamrezael, MasoudSalavati Niasari, Davood Ghanbari and Samira Bagheri (2016), Hydrothermal preparation of silver telluride nanostructures and photo-catalytic investigation in degradation of toxic dyes, Scientific reports 6, article number: 20060
3. Akhil Sreevalsan, Gunhee Kim, Yifan Yu, Sujoy Bandyopadhyay (2025),  $\text{Ag}_2\text{Te}$  Quantum Dots: Emerging Heavy Metal-Free Chalcogenides for near and shortwave Infrared Photodetectors. ACS Appl. Electron. Mater. 7, 21, 9623- 9642
4. Ha Heun Lee, Subin Lee, Geunwoo Hwang, Seungyeon Lee, Suyeon Cho (2024), Vapor- liquid-solid synthesis of  $\text{Ag}_2\text{Te}$  using chemical vapor deposition method, APL Mater. 12, 011123..
5. Nonso Livinus Okoli , Laz Nnadozie Ezenwaka, Ngozi Agatha Okereke, Ifeyinwa Amaka Ezenwa and Nwode Augustine Nwori (2022), Investigation of Optical, Structural, Morphological and Electrical Properties of Electrodeposited Cobalt Doped Copper Selenide ( $\text{Cu}_{1-x}\text{Co}_x\text{Se}$ ) Thin Films, TRENDS IN SCIENCES 2022; 19(16): 5686
6. Shubhendra Gupta, Mukesh Kumar Gupta, Dinesh C. Sharma, Mukesh Kr. Chowrasia and M. K. Banerjee (2023), Structural evolution and thickness-dependant optoelectronic properties in thermally evaporated silver telluride thin films, Indian Journal of Physics, Volume 97, pages 1571–1579
7. High Performance Silver Telluride Thin Films: An Experimental Study S Gupta - 2024 - books.google.com
8. Shubhendra Gupta, Mukesh Kumar Gupta, Dinesh C. Sharma, Mukesh Kr. Chowrasia and M. K. Banerjee (2023), A Study on the Evolution of Structural and Optical Properties in the Thermally Evaporated  $\text{Ag}_2\text{Te}$  Thin Films. Journal of the Institution of Engineers, Volume 104, pages 27–36
9. Alaa M. Abd-Elnaiem, A. M. Abdelraheem, M. A. Abdel-Rahim and Samar Moustafa (2022), Substituting Silver for Tellurium in Selenium–Tellurium Thin Films for Improving the Optical Characteristics, Journal of Inorganic and Organometallic Polymers and Materials, Volume 32, pages 2009–2021
10. Gode, F., Kariper, I. A., Guneri, E., and Unlu, S. (2017). Effect of Complexing Agents on the Structural, Optical and Electrical Properties of Polycrystalline Indium sulphide Thin Films deposited by Chemical Bath Method. *Actaphysicapolonica*, 132(3), 527 – 530.
11. Gode, F. and Unlu, S. (2018). Nickel doping effect on the structural and optical properties of indium sulfide thin films by SILAR, *Open Chemistry*, 16, 757 – 762.
12. Chaudhary, P. and Kumar, V. (2019). Preparation of ZnO thin film using sol-gel dip-coating technique and their characterization for optoelectronic applications. *World Scientific News*, 121, 64 – 71.

13. Ravindranah, K., Prasad, K. D. V. and Rao, M. C. (2016). Spectroscopic and Luminescent Properties of  $\text{Co}^{2+}$  doped tin oxide thin film by Spray Pyrolysis. *Aims Material Science*, 3(3): 796 – 807. Read D. T., J. W. Dally (1993), *J. Mater. Res.* 8, 1542
14. Okorieimoh, C.C., Chime, U., Nkele, A. C., Nwanya, A. C., Madiba, I. G., Bashir, A. K. H., Botha, S., Asogwa, P. U., Maaza, M., and Ezema, F. I. (2019). Room-temperature synthesis and optical properties of nanostructured Ba-Doped ZnO thin films. *Superlattices and Microstructures*, 130, 321 – 331.
15. Anbarasi, M., Nagarethinam, V. S., Baskaran, R. and Narasimman, V. (2016). Studies on the structural, morphological and optoelectrical properties of spray deposited CdS:Pb thin films. *Pacific Science Review A: Natural Science and Engineering*, 18(1), 72 – 77.
16. Hadri, A., Nassiri, C., Chafi, F. Z., Loghmarti, M. and Mzerd, A. (2015). Effect of Acetic Acid Adding on Structural, Optical and Electrical Properties of Sprayed ZnO Thin Films. *Energy and Environment Focus*, 4(1), 12 – 17.
17. Awada, C., Whyte, G. M., Offor, P. O., Whyte, F. U., Kanoun, M. B., Goumri-Said, S., Alshoaibi, A., Ekwealor, A. B. C., Maaza, M. and Ezema, F. I. (2020). Synthesis and Studies of Electrodeposited Yttrium Arsenic Selenide Nanofilms for Opto-Electronic Applications. *Nanomaterials*, 10(8), 1557.
18. Hadri, A., Nassiri, C., Chafi, F. Z., Loghmarti, M. and Mzerd, A. (2015). Effect of Acetic Acid Adding on Structural, Optical and Electrical Properties of Sprayed ZnO Thin Films. *Energy and Environment Focus*, 4(1), 12 – 17.